



geoconvention

Calgary • Canada • May 13-17 2019

Pure P- and S-wave elastic reverse time migration with adjoint state method imaging condition

Jorge E. Monsegny and Daniel O. Trad

University of Calgary

Summary

We implemented an elastic reverse time migration based on a coupled system of pure P- and S-wave particle velocities. The system utilizes finite difference wavefields for P- and S-wave particle velocity in vertical and horizontal directions (v_{px} , v_{pz} , v_{sx} and v_{sz}), and for 2-D displacement divergence and curl (A and B). In contrast with the usual elastic imaging conditions that cross-correlates vertical displacements to obtain the P-wave image and vertical and horizontal displacements to obtain the converted wave image, we devised P- and S-wave imaging conditions using the adjoint state method. The resulting imaging conditions cross-correlate spatial derivatives of A and B wavefields with P- and S-wave displacements. The proposed migration shows a better reflector definition and more balanced amplitudes than the usual vertical and horizontal particle displacement cross-correlations.

Introduction

Reverse time migration (RTM) is a migration method that uses the two-way wave equation and can cope with primaries, multiples and complex structures with all reflector dips (Baysal et al., 1983; McMechan, 1983; Whitmore, 1983). RTM is usually used to migrate P-wave seismic data using the scalar wave equation, however it can also be used with the elastic wave equation.

Regarding the elastic imaging conditions, there are two main approaches based on what you want to obtain. The first approach is to cross-correlate the Cartesian components of the particle velocity/displacement (Chang and McMechan, 1994; Jiang, 2012). In two dimensions the obtained migration images are I_{zz} , I_{zx} , I_{xz} and I_{xx} where the first subscript corresponds to the forward wavefield component and the second to the backward. Due to the seismic mode filter characteristics of the near surface, image I_{zz} could be considered akin to a P-wave migration while I_{zx} could be to a PS-wave migration. However, the practice shows that artifacts due to cross-talk between P and S modes are present (Yan and Sava, 2008).

The other approach is to use a finite difference scheme that directly propagates P- and S-waves. These schemes preserve the P- and S-wave modes amplitude and phase (Duan and Sava, 2015). Du et al. (2017) and Zhang (2019) aim to obtain a single image by using dot product instead of multiplication in the wavefield cross-correlations. Using this method, they avoid rather than correct the PS and SP polarity reversal.

In this report we use the adjoint state method and the pure P- and S-wave finite difference method of Chen (2014) to obtain elastic migration operators that generate P- and S-wave migrated images. The mentioned finite difference scheme also produces P- and S-wave vertical and horizontal displacements that are combined to generate PP and PS migrations.



Theory

The elastic RTM migration is based on the pure P- and S-wave finite difference system of Chen (2014):

$$\begin{aligned}
 v_x &= \frac{\partial u}{\partial t} & v_z &= \frac{\partial w}{\partial t} \\
 v_x &= v_{px} + v_{sx} & v_z &= v_{pz} + v_{sz} \\
 \frac{\partial v_{px}}{\partial t} &= \alpha^2 \frac{\partial A}{\partial x} & \frac{\partial v_{pz}}{\partial t} &= \alpha^2 \frac{\partial A}{\partial z} \\
 \frac{\partial v_{sx}}{\partial t} &= \beta^2 \frac{\partial B}{\partial z} & \frac{\partial v_{sz}}{\partial t} &= -\beta^2 \frac{\partial B}{\partial x} \\
 A &= \frac{\partial u}{\partial x} + \frac{\partial w}{\partial z} & B &= \frac{\partial u}{\partial z} - \frac{\partial w}{\partial x} \\
 \frac{\partial A}{\partial t} &= \frac{\partial v_x}{\partial x} + \frac{\partial v_z}{\partial z} + f_A & \frac{\partial B}{\partial t} &= \frac{\partial v_x}{\partial z} - \frac{\partial v_z}{\partial x} + f_B
 \end{aligned}$$

In this system u and w are the horizontal and vertical particle displacements while v_x and v_z are their time derivatives or particle velocities. However, the system splits these velocities in their P- and S-wave components v_{px} , v_{pz} , v_{sx} and v_{sz} to explicitly evolve them. The wavefields A and B are the divergence and second curl component of the vector $(u, 0, w)$. Although not explicitly addressed by Chen (2014), the P-wave source f_A and S-wave source f_B are injected to wavefields A and B , respectively. Finally, α and β are the P- and S-wave velocities.

It is important to say that this system simulates the coupled P- and S-wave propagation. This means that conversions between modes are possible. For example, when a P-wave propagates, it is entirely contained in the P-wave wavefields v_{px} , v_{pz} and A . When it reaches an interface, the reflected and transmitted S-waves appear in the S-wave wavefields v_{sx} , v_{sz} and B .

We would like to compare the pure P- and S-wave imaging conditions with those proposed for RTM with systems that do not distinguish between pure modes like Levander (1988). This system has vertical v_z and horizontal v_x particle velocities in addition to normal and shear stresses σ_{xx} , σ_{zz} and σ_{xz} . One option for imaging conditions is to take advantage of the near surface that works as a mode filter by making the P-waves almost vertical and the S-waves almost horizontal with the following two equations for PP and PS (Chang and McMechan, 1994; Jiang, 2012):

$$I_{PP} = \int_0^T v_z \hat{v}_z dt, \quad I_{PS} = \int_0^T v_z \hat{v}_x dt$$

where T is the maximum seismogram time and the hat (" $\hat{}$ ") means reverse propagated.



Regarding the P- and S-wave pure mode system, there are also several imaging conditions. Du et al. (2017) propose to perform the dot product between the Cartesian components of the P and S modes to obtain two PP and PS imaging conditions:

$$I_{PP} = \int_0^T (v_{px}, v_{pz}) \cdot (\hat{v}_{px}, \hat{v}_{pz}) dt, \quad I_{PS} = \int_0^T (v_{px}, v_{pz}) \cdot (\hat{v}_{sx}, \hat{v}_{sz}) dt$$

Finally, we propose two imaging conditions for PP and PS that are obtained by the adjoint state method (Feng and Schuster, 2017).

$$I_{PP} = 2\alpha \int_0^T \left(\frac{\partial A}{\partial x}, \frac{\partial A}{\partial z} \right) \cdot (\hat{v}_{px}, \hat{v}_{pz}) dt, \quad I_{PS} = 2\beta \int_0^T \left(\frac{\partial B}{\partial z}, -\frac{\partial B}{\partial x} \right) \cdot (\hat{v}_{sx}, \hat{v}_{sz}) dt$$

In these dot products the backpropagated wavefields are the Cartesian components of particle velocities, while the forward propagated wavefields are spatial derivatives of A and B. The imaging condition also multiplies the cross-correlation by twice the corresponding velocity.

Results

The experiment uses the elastic Marmousi model (Versteeg, 1994). A total of 17 shots evenly spaced over the model top where simulated with receivers along the top horizontal model extension. In this experiment a 20Hz Ricker wavelet was used as source with and without mode separation.

Figure 1 shows the PP migration results. In the left is the vertical displacement RTM that shows less resolution than the other two images. In the right is the vector imaging condition with a very good quality and below is the adjoint state method PP RTM. Figure 2 displays the PS migration results. The vertical-horizontal displacement RTM is on the left. The other two, vector RTM and adjoint state method RTM show more resolution, especially the first one.

Conclusions

Regarding the pure P- and S-wave RTM imaging conditions, the PP and PS dot product generated the best images. These imaging conditions were reported before in (Du et al., 2017) but they use a different finite difference system.

The adjoint state imaging conditions were second place. However, they performed much better than the classical non-pure modes imaging conditions and they do not suffer from PS polarity reversal. PP polarity reversal is still unknown.

Acknowledgements

We would like to express our gratitude to the sponsors of CREWES for continued support. This work was funded by CREWES industrial sponsors and NSERC (Natural Science and Engineering Research Council of Canada).

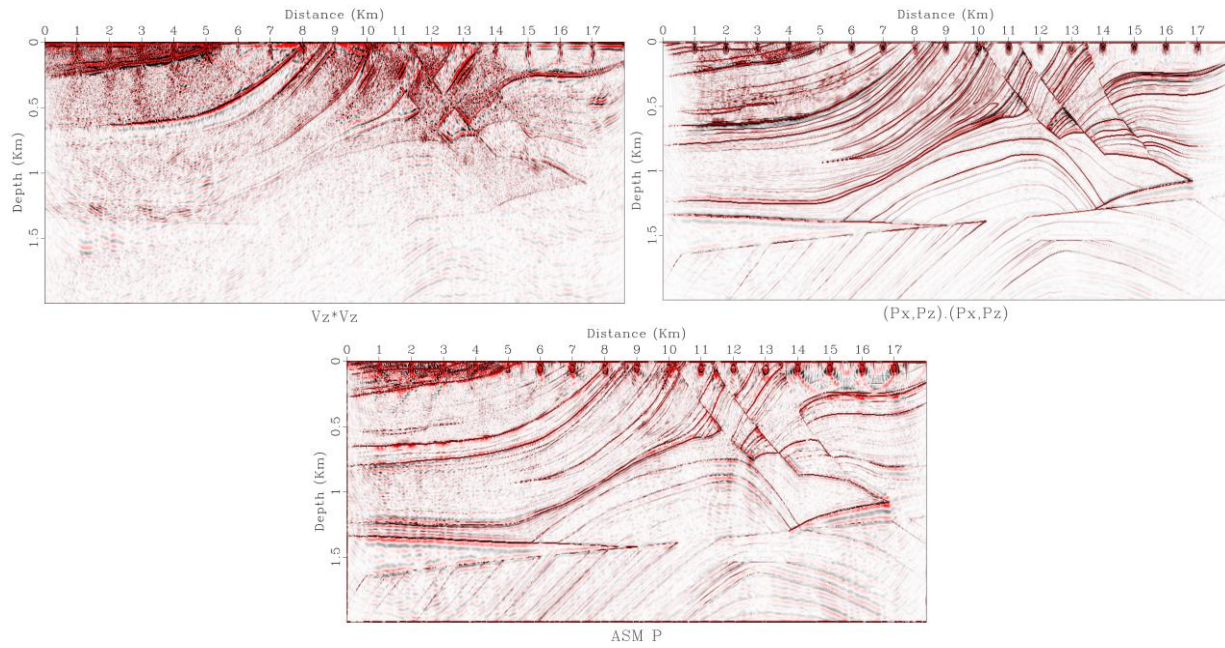


Figure 1. PP RTM results. Above left is vertical displacements RTM. Above right is dot product vector RTM. Below is adjoint state method RTM

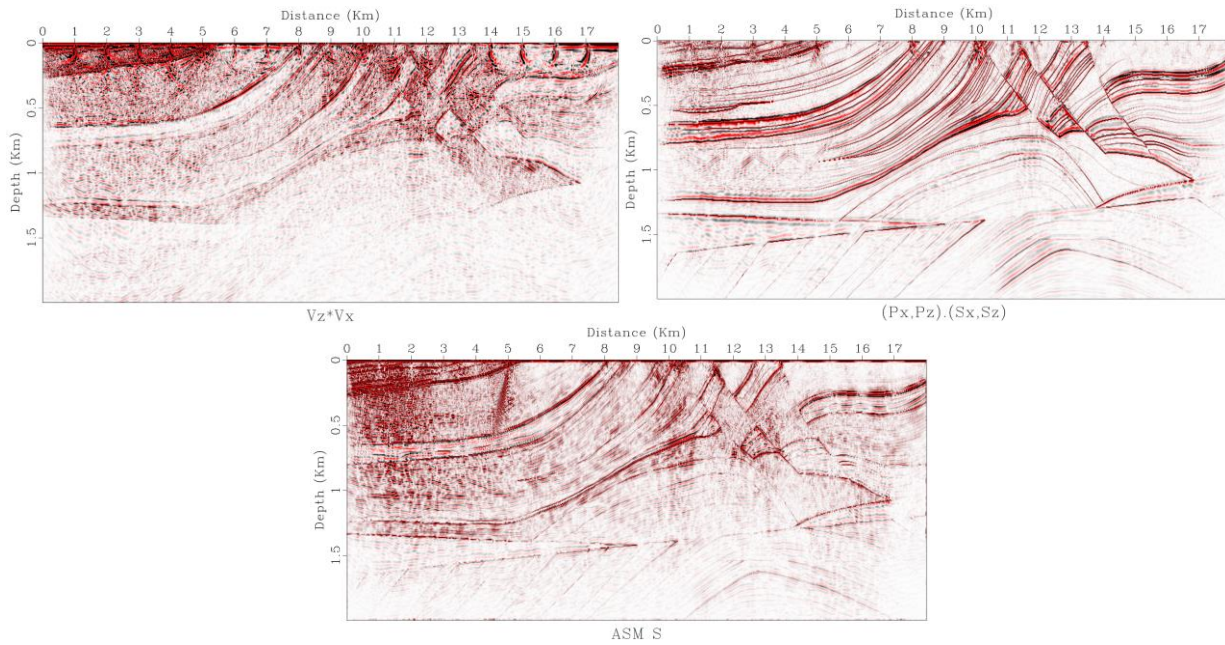


Figure 2. PS RTM results. Above left is vertical-horizontal displacements RTM. Above right is dot product vector RTM. Below is adjoint state method RTM



References

- Baysal, E., Kosloff, D. D., and Sherwood, J. W. C., 1983, Reverse time migration: *GEOPHYSICS*, 48, No. 11, 1514–1524.
- Chang, W., and McMechan, G. A., 1994, 3-d elastic prestack, reverse time depth migration: *GEOPHYSICS*, 59, No. 4, 597–609.
- Chen, K.-Y., 2014, Finite-difference simulation of elastic wave with separation in pure p- and s-modes: *Journal of Computational Methods in Physics*, 14.
- Du, Q., Guo, C., Zhao, Q., Gong, X., Wang, C., and yang Li, X., 2017, Vector-based elastic reverse time migration based on scalar imaging condition: *GEOPHYSICS*, 82, No. 2, S111–S127.
- Duan, Y., and Sava, P., 2015, Scalar imaging condition for elastic reverse time migration: *GEOPHYSICS*, 80, No. 4, S127–S136.
- Feng, Z., and Schuster, G. T., 2017, Elastic least-squares reverse time migration: *GEOPHYSICS*, 82, No. 2, S143–S157.
- Jiang, Z., 2012, Elastic wave modelling and reverse-time migration by a staggered-grid finite-difference method: Ph.D. thesis, University of Calgary.
- Levander, A. R., 1988, Fourth-order finite-difference p-sv seismograms: *GEOPHYSICS*, 53, No. 11, 1425–1436.
- McMechan, G. A., 1983, Migration by extrapolation of time-dependent boundary values: *Geophysical Prospecting*, 31, No. 3, 413–420.
- Versteeg, R., 1994, The marmousi experience: Velocity model determination on a synthetic complex data set: *The Leading Edge*, 13, No. 9, 927–936.
- Whitmore, N. D., 1983, Iterative depth migration by backward time propagation, *SEG Technical Program Expanded Abstracts 1983*: pp. 382-385
- Yan, J., and Sava, P., 2008, Isotropic angle-domain elastic reverse-time migration: *GEOPHYSICS*, 73, No. 6, S229–S239.
- Zhang W. and Shi Y., 2019, Imaging conditions for elastic reverse time migration. *GEOPHYSICS*, accelerated articles.